

Improvement of Relay Link Capacity in a Multi-hop System by using a Directional Antenna in LTE-A Cellular Network

Abstract. This paper introduces a new approach for enhancing relay link quality. Two types of antennas were proposed at the relay node (RN). The first type is the directional antenna, which is directed toward the base station to achieve the maximum relay location range and improve the relay link quality, thereby reducing outage probability by increasing relay link capacity. The second type is the omni-directional antenna, which is used for the exchange of information between the RN and attached users. The optimum relay location was derived, thus ensuring the maximum spectral efficiency and best received signal strength over the relay link and cell edge. An improvement of 32% in spectral efficiency and a difference of -62 dBm to -50dBm in received signal strength at the relay link has been observed while considering Interference from neighboring cells. An ATDI simulator, which manages the digital cartography for the first tier of interference in urban areas, verified the numerical results.

Streszczenie. Opisano metody poprawy transmisji w sieci komórkowej LTE. Zbadano dwie anteny – antenę kierunkową i wielokierunkową. Antena kierunkowa zapewnia najlepszą jakość transmisji, antena wielokierunkowa jest użyta do wymiany informacji między węzłem a użytkownikiem. (Poprawa możliwości transmisji w sieci komórkowej LTE w systemie multi-hop przy wykorzystaniu anteny kierunkowej)

Keywords: Directional antenna, LTE-A, relay, spectral efficiency.

Słowa kluczowe: sieć LTE, antenna kierunkow

Introduction

Relaying improves the coverage of cellular networks in long term evolution advanced by providing high data rate coverage in highly shadowed environments (e.g., indoors) and hotspots, reducing the deployment costs of cellular networks, extending the battery life of user equipment (UE), reducing the overall transmission power of cellular networks, and improving the effectiveness of cell throughput and capacity [1,2].

The relay node (RN) is the intermediate node between the base station (BS) and UE that receives radio frequency signals from the BS. The RN processes these signals and re-sends them to various UEs [3].

An RN wirelessly connects with the BS by relay link .This feature enhances coverage and throughput and decreases costs by circumventing the installation of new BSs and purchase of microwave link equipment. By contrast, UEs are connected to the RN via the access link.

The capacity and coverage at the cell edge remain relatively small because of the low signal-to-interference plus-noise ratio (SINR).The capacity near the BS is better than that near the cell edge; thus, users at the cell edge can cause blocking, and outage probability is high because the number of accepted users is directly proportional to the resources of the service provider [4].

RN performance is restricted by the capacity of the relay link, which carries all the information generated by the RN and users attached to the RN.A relay link can be represented as a bottleneck (Fig.1a). The long distance between the relay location and BS improves the coverage at cell boundaries but degrades the relay link efficiency, thereby increasing outage probability. On the contrary, the approximation of the relay location does not achieve the desired goals for RN deployment. Any improvements in link quality ensure the capacity and required throughput for the growing number of users at the cell boundaries.

A directional antenna (DA) provides signal coverage in a specified direction. The DA improves relay link quality, signal strength, network capacity, and prevents unnecessary interference in the network [5].

In this work, we directed the DA toward the BS to achieve the maximum relay location range. Improving the link quality through the relay link reduces the outage probability and increases the relay link throughput, thereby increasing the number of accepted users. For the access link, we used the omni-directional antenna (OA) to

exchange information between the RN and attached users (Fig.1b). An ATDI simulator was employed to confirm the numerical results transacted with digital cartography in the first tier of interference in urban areas.

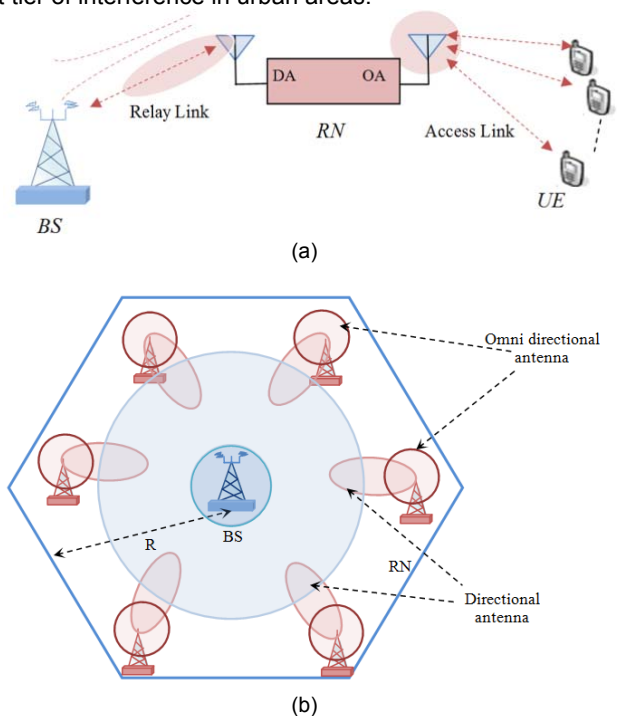


Fig.1.The proposed system model scheme (a) DA and OA (b) proposed model of 6RN deployment

System model

In the cooperative wireless network of Fig. 2, a donor node BS communicates with a user equipment node UE a through RN .Communication happen in two phases. In the first phase, the BS transmits signal X to the relay. The relay processes the received signal with (demodulation and decoding thus modulation and coding) and then retransmits it to the destination in the second phase [4].

The task in this paper is divided in two cases with and without the relaying to explain the effect of the relaying on the system

Capacity without relaying

The downlink received signal at each k user without relay cooperative can be represented as the following equation:

$$(1) Y_{i,k} = \sqrt{P_i} H_{i,k} X_{i,k} + \sum_{j=0}^{N_{cell}} \sqrt{P_j} H_{j,k} X_{j,k} + N_o$$

P_i and P_j are the transmit power of sender BS and neighboring BSs respectively; $H_{i,k}$ and $H_{j,k}$ are the fading channel gain for sender and neighboring cell, respectively; and N_o is AWGN for user .

$$(2) \rho_{i,k} = \frac{P_i |H_{i,k}|^2}{N_o + \sum_{j=0}^{N_{cell}} P_j |H_{j,k}|^2}$$

where $\rho_{i,k}$ is the SINR from the ith link in each single sub-carrier k-UEs. In a severely limited interference scenario, the background noise N_o can be ignored to simplify the calculations [6], so, Eq.2 can be written as:

$$(3) \rho_{i,k} = \frac{P_i G_r G_t D_{i,k}^{-\alpha}}{\sum_{j=1}^N P_j G_r G_t d_{j,k}^{-\alpha}}$$

$$(4) \rho_{i,k} = \frac{P_i L D_{i,k}^{-\alpha}}{\sum_{j=1}^N P_j L_j d_{j,k}^{-\alpha}}$$

where the H is the function of path loss, $|H|^2 = LD^{-\alpha}$, $L = G_r G_t$ is constant depending on the technical characteristics of transmitter and receiver, G_r, G_t is the antenna gains of the transmitter and receiver respectively $D_{i,k}$ and $d_{j,k}$ are the distances from user to donor BS_i and neighbor BS_j respectively, α is the path loss exponent [4,7].

According to [8, 9], the capacity in a single-input single-output LTE system can be estimated by

$$(5) C_i = \min \{ BW_{eff} \log 2(1 + \rho_i / \rho_{eff}), C_{max} \}$$

where C_i is the estimated spectral efficiency in bps/Hz, C_{max} is the upper limit based on the hard spectral efficiency given by 64-quadrature amplitude modulation with the coding rate of 0.753 equal to 4.32 bps/Hz [8,10] . ρ_i is the SINR for each user in the cell, BW_{eff} is the adjustment for the system bandwidth efficiency, and ρ_{eff} is the adjustment for the SINR implementation efficiency.

$\{ BW_{eff}, \rho_{eff} \}$ has the value of {0.56, 2.0} in the downlink and {0.52, 2.34} in the uplink [8]. Capacity distribution practically is represented by two regions. The first region is bordering the BS is known as the satiated capacity which is specified from $0 \rightarrow X_s$, while the other region is determined from $X_s \rightarrow R$, where in this region, the cell capacity represented according to Shannon theory, as shown in Fig. 2.

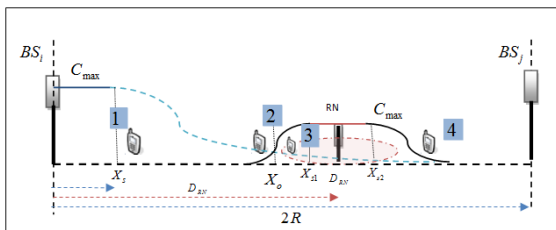


Fig. 2 Proposed node locations.

To calculate the satiated capacity distance X_s , where the level capacity is equal to C_{max} at location (1), as shown in Fig.2, the received signal at UE can be written as

$$(6) Y_{i,x_s} = \sqrt{P_i} H_{i,x_s} X_{i,x_s} + \sum_{j=0}^{N_{cell}} \sqrt{P_j} H_{j,x_s} X_{j,x_s} + N_o$$

The ideal SINR at X_s location is

$$(7) \rho_{ideal} = \frac{P_i L X_s^{-\alpha}}{P_j L_1 (2R - X_s)^{-\alpha}}$$

where L_1 is constant depending on the infrastructure of neighbor BSs. The Error Vector Magnitude (EVM) is a measure of the difference between the ideal symbols and the measured symbols after the equalization [11] thus this difference is called the error vector magnitude. For 64QAM modulation in LTE-A the signal to interference plus noise ratio (ρ_i, X_s) at X_s location is explained as[11];

$$\frac{1}{\rho_{i,X_s}} = \frac{1}{\rho_{max}} + \frac{1}{\rho_{ideal}}$$

where

$$(8) \rho_{ideal} = \frac{P_i L X_s^{-\alpha}}{P_j L_1 (2R - X_s)^{-\alpha}}$$

$$\rho_{i,X_s} = \frac{\rho_{ideal} \rho_{max}}{\rho_{ideal} + \rho_{max}} = \frac{\rho_{max} \frac{P_i L X_s^{-\alpha}}{P_j L_1 (2R - X_s)^{-\alpha}}}{\rho_{max} + \frac{P_i L X_s^{-\alpha}}{P_j L_1 (2R - X_s)^{-\alpha}}}$$

$$X_s = \frac{2R}{1 + \left(\frac{P_i L}{P_j L_1} \right)^{-\frac{1}{\alpha}} (\rho_{i,X_s})^{\frac{1}{\alpha}} - (\rho_{max})^{\frac{1}{\alpha}}}$$

For downlink LTE network the $\rho_{max} = 0.08$ with 64QAM [11]. If we assume that all BSs have the same characteristics in LTE networks, then the distance of satiated region from the BS is

$$(9) X_s = \frac{2R}{1 + (\rho_{i,X_s})^{\frac{1}{\alpha}} - (\rho_{max})^{\frac{1}{\alpha}}}$$

therefore the $X_s = 369.5m$ if $\alpha = 2.7$ for urban area , $\rho_i, X_s = 30dB$ for 64QAM and 2500m radius

Handover location improvement

The relay node and base station are placed at a specific distance from each other, this distance is determines quality of relay link that exchange all information between users and BS through the RN. Handover is a process of transferring UE from base station to relay node depending on the average received signal strength between them. Thus the SINR at UE from the relay is equal to the SINR from BS ; here the user is at a handover point [12].

The distance from the BS to X_o is defined as handover point , as shown in Fig. 3, so , any decrease in the handover distance leads to improvement in relay link.

The distance from relay location D_{RN} to X_o is $D_{RN} - X_o$. Thus, the received signal from the BS at the UE in X_o point can be expressed as

$$(10) Y_{i,X_o} = \sqrt{P_i} H_{i,X_o} X_{i,X_o} + \sqrt{P_{RN}} H_{RN,X_o} X_{RN,X_o} + N_o$$

therefore, SINR at UE in X_o point through direct link is

$$(11) \quad \rho_{i,X_o} = \frac{P_i |H_{i,X_o}|^2}{P_{RN} |H_{RN,X_o}|^2}$$

$$(12) \quad \rho_{i,X_o} = \frac{P_{BS} L X_o^{-\alpha}}{P_{RN} L_r (D_{RN} - X_o)^{-\alpha}}$$

where L_r is the relay node characteristic. The SINR through relay link can be expressed as

$$(13) \quad \rho_{RN,X_o} = \frac{P_{RN} L_r (D_{RN} - X_o)^{-\alpha}}{P_i L X_o^{-\alpha}}$$

In handover point the SINR at UE from BS is equal to the SINR at UE rather than RN as shown in Fig. 3.

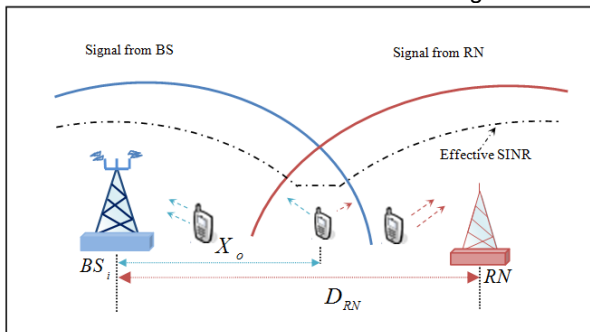


Fig. 3. Handover point performance.

to evaluate the X_o , according to Eqs. (12), (13),

$$(14) \quad \frac{P_i L X_o^{-\alpha}}{P_{RN} L_r (D_{RN} - X_o)^{-\alpha}} = \frac{P_{RN} L_r (D_{RN} - X_o)^{-\alpha}}{P_i L X_o^{-\alpha}}$$

$$X_o = \frac{P_{RN}^{-1} L_r D_{RN}}{\left(L P_i^{-1} + L_r P_{RN}^{-1} \right)}$$

$$X_o = \frac{D_{RN}}{\left(\left(\frac{L_r P_{RN}}{L P_i} \right)^{\frac{1}{\alpha}} + 1 \right)}$$

From eq.(14) the $L_r = G_o G_d$, thus $X_o \propto 1 / G_d$, therefore any increment at the gain of DA RN result in approximated the handover distance and improvement the spectral efficiency where the G_o, G_d is OA gain of UE and DA of RN respectively.

Capacity with relay node

The equations of relay coverage are calculated, where limitations exist between the points presented in Fig. 2. The received signals at UE in locations 2 and 3 (as indicated in Fig. 2) can be represented as

$$(15) \quad Y_{RN,2} = \sqrt{P_{RN}} H_{RN,2} X_{RN,2} + \sqrt{P_i} H_{i,2} X_{i,2} + N_o$$

$$(16) \quad Y_{RN,3} = \sqrt{P_{RN}} H_{RN,3} X_{RN,3} + \sqrt{P_i} H_{i,3} X_{i,3} + N_o$$

The SINR for these two locations is

$$\rho_{RN,2} = \frac{L_r P_{RN} |H_{RN,2}|^2}{P_i L |H_{i,2}|^2}, \quad \rho_{RN,3} = \frac{P_{RN} |H_{RN,3}|^2}{P_i |H_{i,3}|^2}$$

$$(18) \quad \rho_{RN,2} = \frac{P_{RN} L_r (D_{RN} - D_i)^{-\alpha}}{P_i L D_i^{-\alpha}}$$

$$(19) \quad C_{RN,2} = \min \left\{ BW_{eff} \log_2 \left(1 + \frac{P_{RN} L_r (D_{RN} - D_i)^{-\alpha}}{P_i L \rho_{eff} D_i^{-\alpha}} \right), C_{Rmax} \right\}$$

For $X_o < D_i < X_{s1}$

$$(20) \quad C_{RN,3} = \min \left\{ BW_{eff} \log_2 \left(1 + \frac{P_{RN} L_r (D_{RN} - D_i)^{-\alpha}}{P_i L \rho_{eff} D_i^{-\alpha}} \right), C_{Rmax} \right\}$$

For $X_{s2} < D_i < R$ otherwise equal C_{Rmax} , where C_{Rmax} is the maximum spectral efficiency of relay that depends on the SINR and adaptive modulation scheme.

Optimum relay location

In this section, the issue of the optimum placement of the relay node deployment in a dual-hop network over LTE-A cellular networks will be addressed as well as the maximum throughput.

Optimum relay location according outage probability

Outage is defined as the event in which the received signal to noise ratio SNR falls below a certain threshold γ_{th} [4]. The received signal at the relay and access link is expressed as the following:

$$(21) \quad Y_{i,RL} = \sqrt{P_i} H_{i,RN} X_{t1} + \sum_{j=0}^{N_{cell}} \sqrt{P_j} H_{j,k} X_{t1} + N_o$$

$$(22) \quad Y_{RN,i} = \sqrt{P_{RN}} H_{RN,k} X_{t2} + \sum_{j=0}^{N_{cell}} \sqrt{P_j} H_{j,k} X_{t2} + N_o$$

where $H_{i,RN}$ and $H_{RN,k}$ are the channel gains for relay and access link, respectively. The SINR at the relay link is

$$(23) \quad \gamma_{RL} = \frac{P_i |H_{i,RN}|^2}{N_o + \sum_{j=0}^{N_{cell}} P_j |H_{j,RN}|^2}$$

The SNR at the access link is

$$(24) \quad \gamma_{access} = \frac{P_{RN} |H_{RN,k}|^2}{N_o + \sum_{j=0}^{N_{cell}} P_j |H_{j,k}|^2}$$

The outage probability of these links is defined as

$$(25) \quad P_{o,RL} = P_r(\gamma_{RL} < \gamma_{th}) \approx \frac{\gamma_{th}}{\gamma_{RL}}$$

$$P_{o,RL} = P_r(\gamma_{RL} < \gamma_{th}) = \left(1 - e^{-\frac{\gamma_{th}}{\gamma_{RL}}} \right)$$

and

$$e^{-\frac{\gamma_{th}}{\gamma_{RL}}} \approx \left(1 - \frac{\gamma_{th}}{\gamma_{RL}} \right) \Rightarrow P_{o,RL} \approx 1 - 1 - \frac{\gamma_{th}}{\gamma_{RL}}$$

then

$$(26) \quad P_{o,RL} = P_r(\gamma_{RL} < \gamma_{th}) \approx \frac{\gamma_{th}}{\gamma_{RL}}$$

on the same procedure

$$(27) \quad P_{o,access} = P_r(\gamma_{access} < \gamma_{th}) \approx \frac{\gamma_{th}}{\gamma_{access}}$$

The outage probability for a multi-hop link can be expressed as

$$(28) P_{o,MH} = \frac{\gamma_{th} \left(N_o + \sum_{j=0}^{N_{cell}} P_j |H_{j,RN}|^2 \right)}{P_i |H_{i,RN}|^2} + \frac{\gamma_{th} \left(N_o + \sum_{j=0}^{N_{cell}} P_j |H_{j,k}|^2 \right)}{P_{RN} |H_{RN,k}|^2}$$

$$(29) P_{o,MH} = \frac{\gamma_{th} \left(N_o + \sum_{j=0}^{N_{cell}} P_j |H_{j,RN}|^2 \right) D_{RN}^\alpha}{P_i L} + \frac{\gamma_{th} \left(N_o + \sum_{j=0}^{N_{cell}} P_j |H_{j,k}|^2 \right) (R - D_{RN})^\alpha}{L_r P_{RN}}$$

For simplify the calculation suppose the $|H_{j,k}|=|H_{j,RN}|=|H_o|$ [13] where the distance between the RN and UE is very close compared to distances with neighboring BSs. Thus the optimum location of the relay for overall cell of two multi-hop links can be obtained by using the mathematics of convex optimization [14]. Thus, taking the first derivative of Eq. (30) with respect to D_{RN} and setting it to zero, then

$$(30) \frac{\Delta P_{o,MH}}{\Delta D_{RN}} = \alpha L_r P_{RN} D_{RN}^{(\alpha-1)} - \alpha L P_i (R - D_{RN})^{(\alpha-1)}$$

$$\alpha (L_r P_{RN})^{\frac{1}{\alpha-1}} D_{RN}^{\frac{1}{\alpha-1}} - \alpha (L P_i)^{\frac{1}{\alpha-1}} (R - D_{RN}) = 0$$

We can obtain the optimum location as

$$(31) D_{RN} = \frac{R (L P_i)^{1/(\alpha-1)}}{(L P_i)^{1/(\alpha-1)} + (L_r P_{RN})^{1/(\alpha-1)}}$$

Optimum relay location according handover

The optimum location of relay at the cell edge between two locations of the user when ($D_i=X_o$) and ($D_i=R$) and are used as the relay capacity equations can be obtained through the following:

$$(32) \frac{(D_{RN} - X_o)^{-\alpha}}{X_o^{-\alpha}} = \frac{(R - D_{RN})^{-\alpha}}{R^{-\alpha}}$$

$$(33) X_o (R - D_{RN}) = R (D_{RN} - X_o)$$

Substituting (14) in (33), we obtain

$$(34) \frac{2D_{RN}R}{1 + \left(\frac{L_r P_{RN}}{L P_i} \right)^{1/\alpha}} - \frac{D_{RN}^2}{1 + \left(\frac{L_r P_{RN}}{L P_i} \right)^{1/\alpha}} - R D_{RN} = 0$$

$$(35) \frac{2R - D_{RN}}{1 + \left(\frac{L_r P_{RN}}{L P_i} \right)^{1/\alpha}} = R$$

then

$$(36) D_{RN} = R \left(1 - \left(\frac{L_r P_{RN}}{L P_i} \right)^{1/\alpha} \right)$$

Simulation calculation

The propagation of a radio wave is a complex and less predictable process if the transmitter and receiver properties are considered in channel environment calculations. The process is subjected by reflection, diffraction, and scattering, the intensities of which vary under different environments at different instances.

The ATDI simulator was used to demonstrate the mathematical results for relay link improvement therefore the propagation model for this simulator between the nodes can be expressed as the following equation:

$$(37) P_r = P_t + G_t + G_r - L_{prop} - L_t - L_{re} \quad [\text{dB}]$$

where P_t indicates the power at the transmitter and P_r is the power at the receiver; L_t and L_{re} express the feeder losses; and L_{prop} is the total propagation loss formulated as

$$(38) L_{prop} = L_{fsd} + L_d + L_{sp} + L_{gas} + L_{rain} + L_{clut}$$

where: L_{fsd} : free space distance loss, L_d : diffraction loss, L_{sp} : sub path loss, L_{gas} : attenuation caused by atmospheric gas, L_{rain} : attenuation caused by hydrometeor scatter, and L_{clut} : cutter attenuation.

This equation explains the link budget. The link budget is determined by all the gains and losses in the path, which is opposite the transmitted signal to reach the receiver. A link is created by three related communication entities: transmitter, receiver, and a channel between them. The medium introduces losses caused by suction in the received power, as shown in Fig. 4.

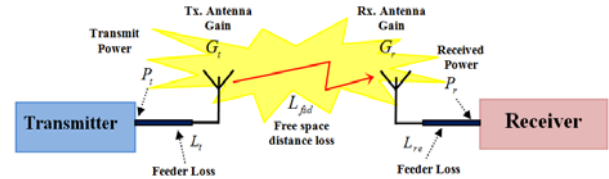


Fig. 4 Link budget scheme

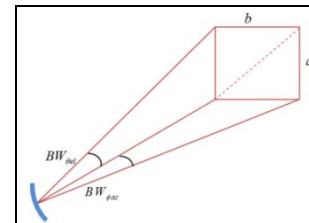


Fig. 5 Antenna Aperture

Antenna type

The DA is used at the RN and is directed toward the BS to improve the link quality and accommodate the most number of users associated through the relay node.

The gain or directivity of an antenna is the ratio of the radiation intensity in a given direction to the average radiation intensity of all directions. Assuming that the pattern of the antenna is uniform, the gain is equal to the area of the isotropic sphere ($4\pi r^2$) divided by the sector (cross section):

$$G_d = \frac{\text{Area of Sphere}}{\text{Area of Antenna Pattern}}$$

$$G_d = \frac{4\pi}{BW_{\phi_{az}} BW_{\phi_{el}}} = \frac{4\pi}{\sin(\phi_{az}) \sin(\theta_{el})}$$

where $BW_{\phi_{az}}$ and $BW_{\phi_{el}}$ are the azimuth angle and beam width elevation in radians, respectively; ϕ_{az} and θ_{el} are the azimuth and elevation angle, respectively (Fig.5) [15]. The increment in gain for the DA depends on the azimuth angle rather than on the OA if the elevation angle is fixed (Eq. (37)).

A parabolic antenna with model (ITU-R F.1245)[16] was used in the simulation test as a DA with variable gain, the antenna pattern was plotted with a 34° elevation angle and 72° azimuth angle according to [15,16]. as shown in Fig. 6. Fig.7 shows four different cases of gain values for radiation power distribution over urban areas by using the ATDI simulator. DA provides the radiation power directed at certain azimuth angle, which increases with increasing input power and antenna gain value (Fig.7).

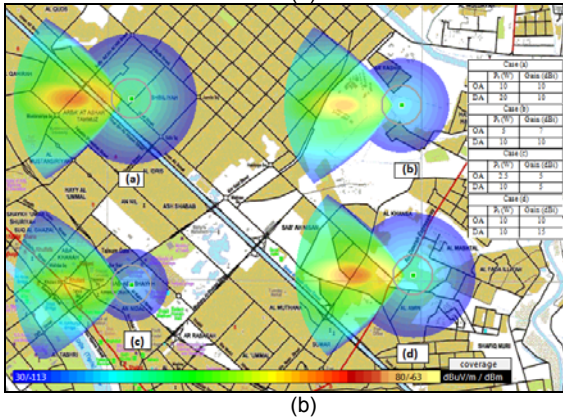
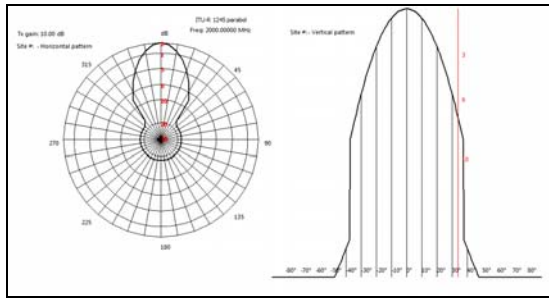


Fig.7 (a) gain antenna pattern distribution azimuth and elevation (b) EIRP distribution over real digital cartography with different gain and transmitted power

Results and Discussion

In this section, we explain and compare the numerical results by using the ATDI simulator, which uses a real digital cartographic representation of an urban area that is approximately 176.7km².

Fig. 8 illustrates the spectral efficiency versus cell radius indicated in Eq. (5). The interference of the first tier and frequency reuse are considered in this simulation, where the simulated parameters (Table 1) are chosen according to [17]. The SINR close to the BS is better than the cell boundaries; thereby, the spectral efficiency at the cell boundaries is reduced because of link budget degradation. The level of saturated regions from the center BS to X_s depends on the type of modulation and coding, which depends on the SINR (Eqs.(5) and (8)).

The numerical and simulation curves are the results of the optimal relay location (Eqs. (30) and (36)), where one OA is used at the RN(Fig.9). The spectral efficiency at the cell edge improves from 0.6 bps/Hz to 1.45 bps/Hz after relay deployment and 25% overall cell improvement.

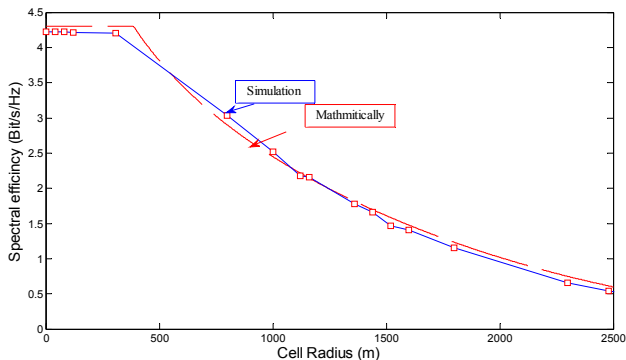


Fig.8 Spectral efficiency versus the cell radius for numerical and ATDI simulation results

Fig. 10 explains the changes of handover distance with the gain of DA at RN according to Eq.(14), where an increasing antenna gain leads to decreasing handover

distance, thereby improving relay link. This improvement in handover distance depends on the path loss exponent (Fig.10).

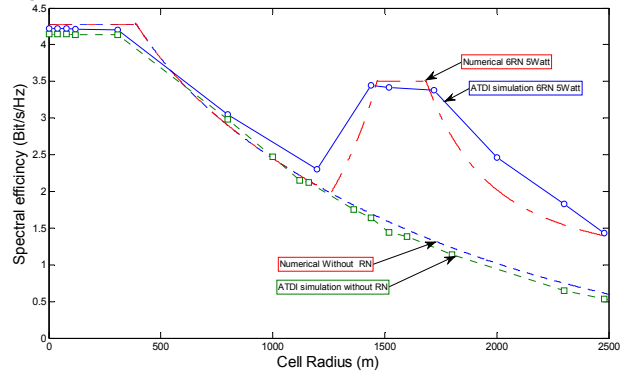


Fig.9 Spectral efficiency versus the cell radius after using 6RN each one 5watt for numerical and ATDI simulation results

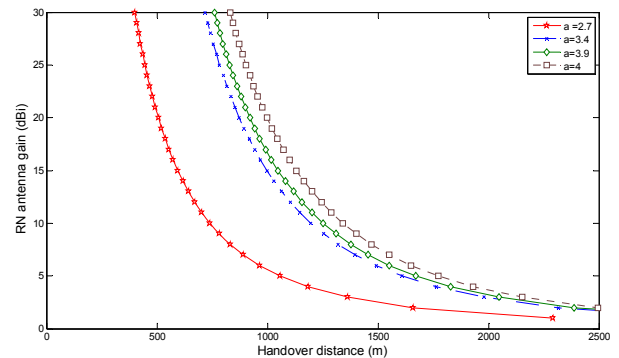


Fig.10.Handover distance versus with the variation gain of directional antenna

The results of the spectral efficiency versus the cell radius with the proposed model are illustrated in Fig.11 by using two types of antenna: a DA directed toward the BS and an OA for information exchange between users and the RN.

Table 1. Simulation Parameters

Carrier Frequency GHz	2
Bandwidth	1.4 MHz
Number of BS	7
Antenna height of BS	25 (m)
Antenna gain of BS	17 dBi
Type of antenna of BS	OA
Transmitted power of BS	40W
Number of (RBs)	6
Modulation and coding schemes	64QAM code (0.625,0.6) 16QAM code 0.8 [8]
Radius of cell	2500m
Type of antenna of RN	OA & DA type ITU R-1245
Antenna height of RN	25 (m)
Antenna gain of RN	(5,10) dBi
Transmitted power of RN	(10,5,2.5)Watt
Number of RNs in cell	6
Number of UE	1
Antenna height of UE	1.5 m
Antenna gain of UE	0 dBm Omni-Directional type
Coverage threshold	-30dBm

Three different cases of gain and RN transmitted power are explained in Fig.11 and summarized in Table 2. Cases 1 and 2 result in improvements in spectral efficiency but consume extra power at the DA. Case 3 exhibits the best solution for improving the relay link; that is, total power is divided between the antennas to prevent extra power consumption (Fig.11 and Table 2.).

Table 2. Proposed Scheme

case	Power (Watt)		Gain (dBi)		Improvement %
	OA	DA	OA	DA	
1	5	5	7	10	37
2	5	5	7	5	29.3
3	2.5	2.5	7	10	32
4	5	--	7	--	25.5
5	--	5	--	10	Not practically

The three different cases of gain and RN transmitted power are explained in Fig.11 and summarized in Table 2. to improve the relay link. The cases one and two are give the improvement in spectral efficiency but they are consume the extra power at DA .The third case is best solution to improve the relay link where total power is divided between the antennas and prevents the consumption of extra power as shown in Fig.11 and Table 2.

The enhancement of spectral efficiency at the relay link according to handover point is from 1.99 bps/Hz to 2.909 bps/Hz compared with the OA. This improvement is a result of the enhancement of the link quality between the RN and BS, thus increasing the number of active users at the cell boundaries and reducing outage probability at the relay link. This proposed scheme increases the overall cell spectral efficiency approximately to 32% (Fig.11).

An ATDI simulator verified the numerical results of the proposed model, which handles several propagation loss parameters according to Eq.(37) with consideration to the digital cartography of the urban area.

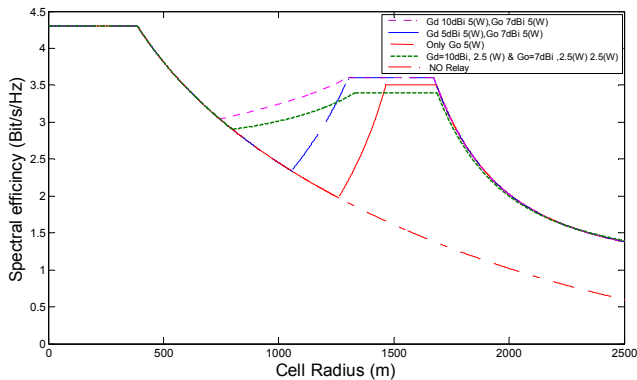
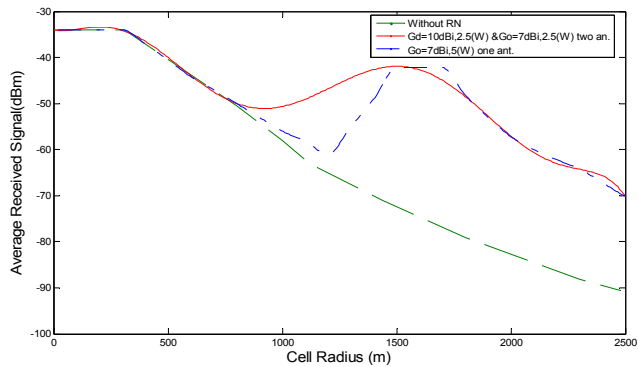
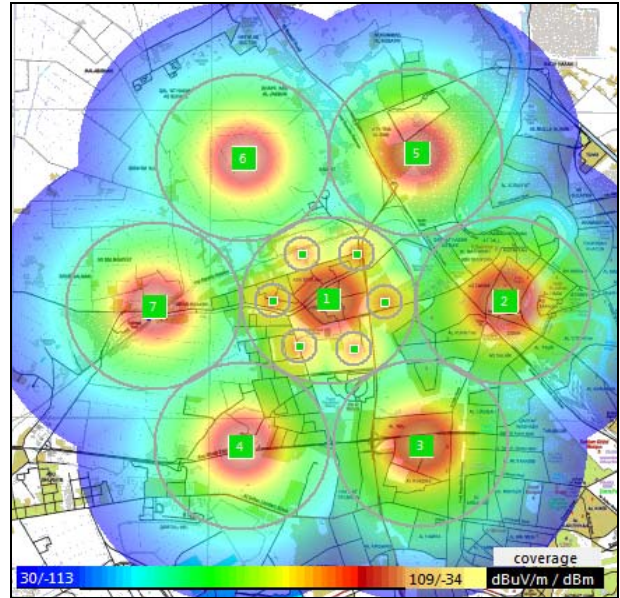


Fig.11. Spectral efficiency of proposed schemes over cell radius (a) of four proposed schemes (b) best proposed scheme

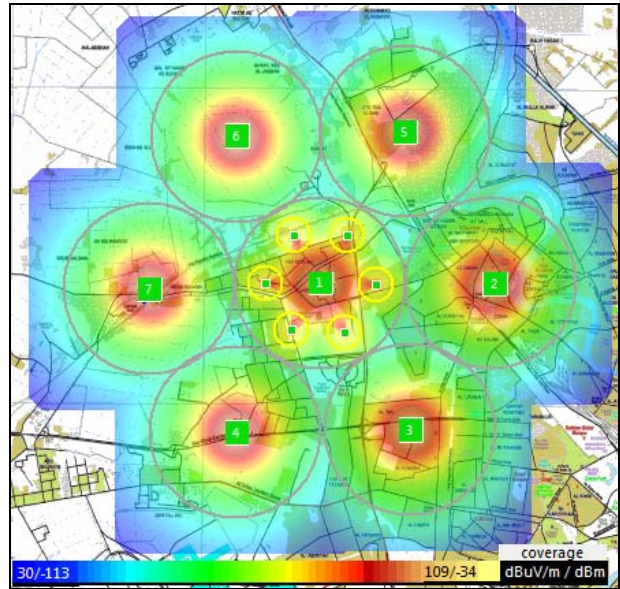
Fig.12a shows the average received signal strength versus the cell radius for the proposed relay location by using two types of antenna proposed in the mathematical model. The two types of antennas (i.e., DA and OA) improve the relay link quality, increase the received signal strength for each active user, and solve the frequent communication interruptions caused by weak signals.



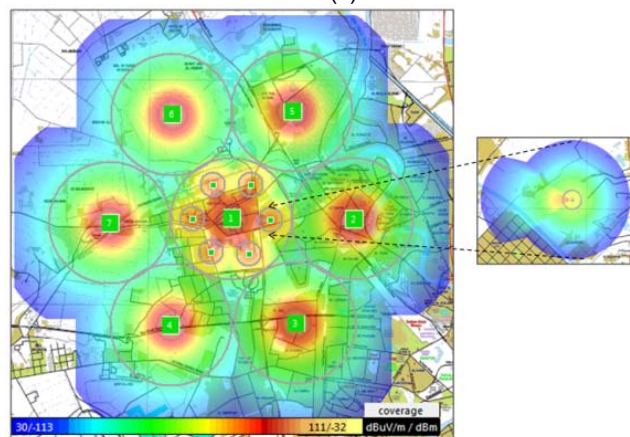
(a)



(b)



(c)



(d)

Fig. 12 Received signal strength versus the distance with a real digital cartographic of an urban city, (a) simulation representation of received signal strength at UE for a proposed RN antenna, (b) chromatic scheme of coverage area distribution for 6RN case 4, (c) chromatic scheme of coverage area distribution for 6RN case 5 (d) chromatic scheme of coverage area distribution for 6RN case 3.

Fig. 12b illustrates the chromatic scheme of the signal strength distribution in Case 4 (Table 2) by proposing six RN in cell. Fig. 12c explains the chromatic scheme of the signal strength distribution for ITU R-1245, which is directed toward the main BS as shown in Case 5 (Table 2). The relay link is improved regardless of the improvements in user link. The best solution is shown in Fig. 12d (i.e., Case 3), where the chromatic scheme signal strength has a fair overall distribution cell while consuming the same RN transmitted power.

Conclusion

We proposed a new approach for solving the relay link problem by maximizing the spectral efficiency at the relay link. In which the link quality in the multi-hop system had been improved and the received signal strength for each active user had been modified also, thereby increasing the number of accepted users in the main network. We derived the optimum relay placement to enhance the coverage and throughput at the cell edge region. The maintaining of link quality provided more flexibility in deploying RNs close to cell boundaries, thereby improving coverage area. An improvement of 32% in spectral efficiency and a difference of -62 dBm to -50dBm in received signal strength at the relay link has been observed while considering Interference from neighboring cells. An ATDI simulator verified the numerical analysis which manages the digital cartography of urban area

REFERENCES

- [1] J. Adhab, A. Yahya, R. B. Ahmad, Performance Enhancement of LTE-A a Multi-Hop Relay Node by Employing Half-Duplex Mode, *IJCSI*, Vol. 9, Issue 3, No 3, May 2012, 73-78.
- [2] Xiao Jie, Gengxin Zhang, Guozhen Zang, Research on Cooperative Diversity in Mobile Satellite Communication System, *Przeegląd Elektrotechniczny*, R. 87 NR 11/2011, 305-309
- [3] Yafeng Wang, Meng Li, Wei Xiang, Graph Based Interference Coordination for Relay Networks, *Przeegląd Elektrotechniczny*, R. 88 NR 1b/2012, 88-91.
- [4] Aleksandra M. Cvetković, Goran T Đorđević, Mihajlo Č. Stefanović, Outage probability of dual-hop semi-blind relaying with interference at the relay, *Przeegląd Elektrotechniczny*, R. 88 NR 12a/2012, 325-327.
- [5] Su Yi, Ming Lei, Backhaul Resource Allocation in LTE-Advanced Relaying Systems, *IEEE wireless communication and networking conference*, 2012, 1217-1221.
- [6] Farooq Khan, LTE for 4G Mobile Broadband Air Interface Technologies and Performance. Cambridge University Press, 2009, 408-413.
- [7] Simon R. Saunders, Antennas and Propagation for Wireless Communication Systems, *John Wiley and Sons*, 2nd edition LTD, England, 2007, 90-94.
- [8] Y. Wang, W. Na, I. Kovács, F. Frederiksen, A. Pokhariyal, K. Pedersen, T. Kolding, K. Hugi, and M. Kuusela, "Fixed Frequency Reuse for LTE-Advanced Systems in Local Area Scenarios" in Proc. *Vehicular Technology Conf.*, VTC2009-Spring. IEEE 69th, 2009, 1-5.
- [9] S. Wang, J. Wang, J. Xu, Y. Teng, K. Horneman, "Cooperative component carrier (Re-)selection for LTE-Advanced femtocells" in Proc. *Wireless Communications and Networking IEEE Conference (WCNC)*, 2011, 629 - 634.
- [10] F. Gordejuela-Sanchez, J. Zhang, Member, LTE Access Network Planning and Optimization: A Service-Oriented and Technology-Specific Perspective, *IEEE Communications Society proceedings*, 2009
- [11] S. Sesia, B. Matthew, and T. Issam, LTE, the UMTS long term evolution: from theory to practice, 2nd edition John Wiley & Sons, Feb 2011, 460-466.
- [12] R. Hussain, S. A. Malik, S. Abrar, R. A. RIAZ, S. A. KHAN, Minimizing Unnecessary Handovers in a Heterogeneous Network Environment, *Przeegląd Elektrotechniczny*, R. 88 NR 6/2012, 300-303.
- [13] Mylene Pischella and Didier Le Ruyet, "Optimal Power Allocation for the Two-Way Relay Channel with Data Rate Fairness" *IEEE Communications Letters*, VOL. 15, NO. 9, September 2011, 959-961.
- [14] Stephen Boyd, Lieven Vandenberghe, *Convex Optimization*. Cambridge university press, Seventh printing with corrections, 2009, 68-72.
- [15] Daniel M. Dobkin, *The RF in RFID Passive UHF RFID in Practice*, Newnes is an imprint of Elsevier, 30 Corporate Drive, Suite 400, Burlington, MA 01803, USA, 20, 86-100
- [16] F. Series, Mathematical model of average and related radiation patterns for line-of-sight point-to-point radio-relay system antennas for use in certain coordination studies and interference assessment in the frequency range from 1 GHz to about 70 GHz, *Recommendation ITU-R F.1245-1*, 2000
- [17] 3GPP TS 36.104 "Base Station (BS) radio transmission and reception", Technical report, 2007

Authors: Mr. Jaafar .A. Aldhaibani worked with the Motorola Company as a system engineer for communication. He also worked with ATDI Company for RF planning communication sites (IC telecom software). Now, he is studying to earn his Ph.D. degree Email: jaffar_athab@yahoo.com .Dr.A.Yahya is Currently, he is working in the School of Computer and Communication Engineering, Universiti Malaysia Perlis (UniMAP) Email abidum@gmail.com ,Prof. R.B.Ahmad is currently the Dean in the School of Computer and Communication Engineering and the Head of the Embedded Computing Research Cluster Email badli@unimap.edu.my
The correspondence address is: e-mail: jaafar_athab@yahoo.com